ISSN 1063-7710, Acoustical Physics, 2016, Vol. 62, No. 2, pp. 143–150. © Pleiades Publishing, Ltd., 2016.

CLASSICAL PROBLEMS OF LINEAR ACOUSTICS AND WAVE THEORY

Study of Thermoviscous Dissipation on Axisymmetric Wave Propagating in a Shear Pipeline Flow Confined by Rigid Wall. Part II. Numerical Study[1]

Xiaoqian Chen[a], Yong Chen[a], Yiyong Huang[a], Yuzhu Bai[a], Dengpeng Hu[b], and Shaoming Fei[c]

[a] *College of Aerospace Science and Engineering, National University of Defense Technology, 410073 Changsha, China*

[b] *Air Force Early Warning Academy, 430019 Wuhan, China*

[c] *Electronic Experiment Center, Chengdu University of Information Technology, 610000 Chengdu, China*

e-mail: literature.chen@gmail.com; yiyong_h@sina.com; chenxiaoqian@nudt.edu.cn; baiyuzhu@gmail.com; hudengpeng@163.com; fsm@cuit.edu.cn

Received February 25, 2014

Abstract—Axisymmetric acoustic wave propagating in a shear pipeline flow confined by a rigid wall is studied in the two-part paper. The effects of viscous friction and thermal conduction on the acoustic wave propagating in the liquid and perfect gas are respectively analyzed under different configurations of acoustic frequency and shear mean flow. In Part 2 of this paper, comprehensive analysis of the effects of shear mean flow and acoustic frequency on the features (relative phase velocity and attenuation coefficient) of the acoustic wave are numerically addressed in cases of water and perfect gas respectively. Comparisons between the non-isentropic and isentropic models are provided in details. Meanwhile, discussions of the thermoviscous effects on the acoustic wave between water and perfect gas are given.

Keywords: thermoviscous dissipation, duct acoustics, shear flow, relative phase velocity, attenuation coefficient

DOI: 10.1134/S1063771016020160

INTRODUCTION

Wave propagation in the pipeline flow is of great interest in both theoretical and industrial applications [1–6]. In the aircraft engineering, for example, particular considerations are placed on the prediction and attenuation of engine noises [7–13]. The prediction of aeroacoustic features is also important in the catalytic converter design of a transport system [14, 15]. In the ultrasonic pipeline flow measurement [16, 17], accurate prediction of ultrasonic wave propagation is of great importance on the improvement of measurement performance.

In the first part [18], mathematical descriptions of axisymmetric wave propagation in the presence of a shear mean flow confined by a circular rigid wall are formulated. The proposed models of the non-isentropic and isentropic acoustic waves relax the constraint of Zwikker and Kosten theory which makes sense in the case that only the fundamental mode exists. As a result, the features of high-order acoustic modes can be analyzed using proposed models. Based on Fourier–Bessel theory, the first part of this paper gives solutions to the acoustic models in the liquid and perfect gas respectively and then presents a general procedure of iteratively calculating the dimensionless wavenumber. The validity of the proposed models is presented as well.

In this part, the authors concentrate on the analysis of wave propagation in the presence of high-order modes based on the theoretical contributions in the first part. Particular considerations are placed on the relative phase velocity and attenuation coefficient under the effects of the flow profile, acoustic frequency and thermoviscous dissipation. Meanwhile, the difference of non-isentropic and isentropic models are highlighted in the liquid and perfect gas respectively. It should be noticed that the pipeline radius also changes the features of the acoustic wave which can be easily handled using proposed models. Readers can consult similar analysis in the case of a uniform flow [19].

THE EFFECT OF FLOW PROFILE

This section deals with the influence of flow profile on the acoustic wave propagating forwardly and backwardly in the fluid confined by a circular rigid wall. Specifically, numerical calculations of wave propagating in liquid are based on water with the coefficients

[1] The article is published in the original.

The coefficients of the third-order polynomial function of sound speed

α_0	α_1	α_2	α_3
1449.2	4.6	−0.055	0.00029

being the density $\rho_0 = 1000$ kg/m^3, special heat ratio $\gamma = 1$, volume thermal expansion $\beta = 0.207 \times 10^{-3}$ 1/°C, heat coefficient at constant pressure $c_p = 4181.3$J/(kg K), thermal conductivity $\kappa_{th} = 0.5984$ W/(k m), shear viscosity $\eta = 1 \times 10^{-3}$ kg/(s m) and bulk viscosity $\zeta = 2.4\eta$. Meanwhile, the coefficients used in the case of perfect gas are $\rho_0 = 1.225$ kg/m^3, $\gamma = 1.4$, $c_p = 1184$ J/(kg K), $\kappa_{th} = 0.0786$ W/(k m), $\eta = 4.15 \times 10^{-5}$ kg/(s m) and the gas constant $R_0 = 287$J/(kg K). The steady temperature of the wall and the pipeline radius are $T_{wall} = 293$ K (20°C) and $R = 0.1$ m. Numerical calculations are concentrated on the wave propagating in the laminar flow with the profile

$$M(x) = 2\overline{M}(1-x^2), \tag{1}$$

where $\overline{M}$ is the averaged mean Mach number. According to the mathematical formulation in the first part, the steady temperature in water satisfies

$$\frac{1}{x}\frac{d}{dx}\left(x\frac{dT_0}{dx}\right) = -\frac{\eta\beta T_0\bar{c}_0^2}{\kappa_{th}}M\frac{d}{dx}\left(x\frac{dM}{dx}\right) - \frac{\eta\bar{c}_0^2}{\kappa_{th}}\left(\frac{dM}{dx}\right)^2, \tag{2}$$
$$T_0(x=1) = T_{wall},$$

while the corresponding dynamic equation in the perfect gas is

$$\frac{1}{x}\frac{d}{dx}\left(x\frac{dT_0}{dx}\right) = -\frac{\eta\bar{c}_0^2}{\kappa_{th}}M\frac{d}{dx}\left(x\frac{dM}{dx}\right) - \frac{\eta\bar{c}_0^2}{\kappa_{th}}\left(\frac{dM}{dx}\right)^2, \tag{3}$$
$$T_0(x=1) = T_{wall}.$$

In water, the adiabatic sound speed c_0, which is approximately a function of the steady temperature, can be written as a third-order polynomial expression with [16]

$$c_0 = \sum_{n=0}^{3}\alpha_n(T_0 - 273)^n, \tag{4}$$

where $(T_0$—$273)$ is restricted to be in the range 0–95°C and the coefficients α_n are listed in table.

It should be noticed that under the current configurations, some high-order modes can turn out and propagate in the fluid. However, present paper analyzes the features of the first two modes propagating in water and perfect gas. Physically speaking, the existence of a specific acoustic mode is determined by the corresponding cut-off frequency. In the case of an inviscid fluid, discussions of the cut-off frequency were summarized by Boucheron et al. [20]. Furthermore, present authors [21] investigated the problem in the case of a viscous fluid on the neglect of thermal conduction. Frankly speaking, it may be hard to calculate the cut-off frequency of a specific acoustic mode under the effect of thermoviscous dissipation, however, the existence of the possible acoustic modes can be verified by plotting the absolute value of det($\mathbf{G}(K)$) shown in part 1 as a function of the axial

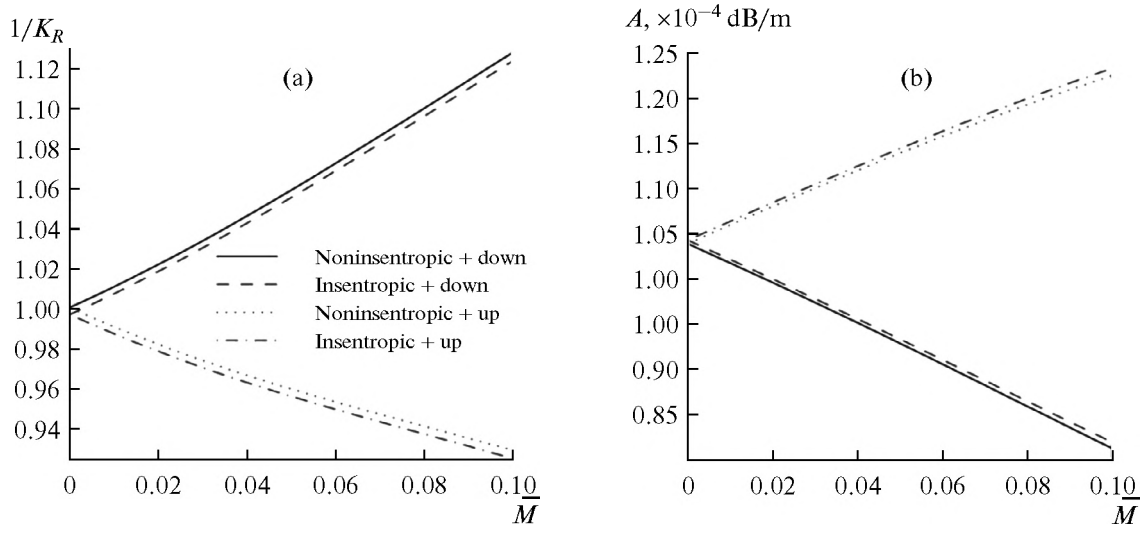

Fig. 1. The effect of flow profile on the relative phase velocity and attenuation coefficient of the fundamental non-isentropic and isentropic acoustic waves propagating in a tube filled with water. (a) relative phase velocity; (b) attenuation coefficient. The legends are placed in Fig. 1a.

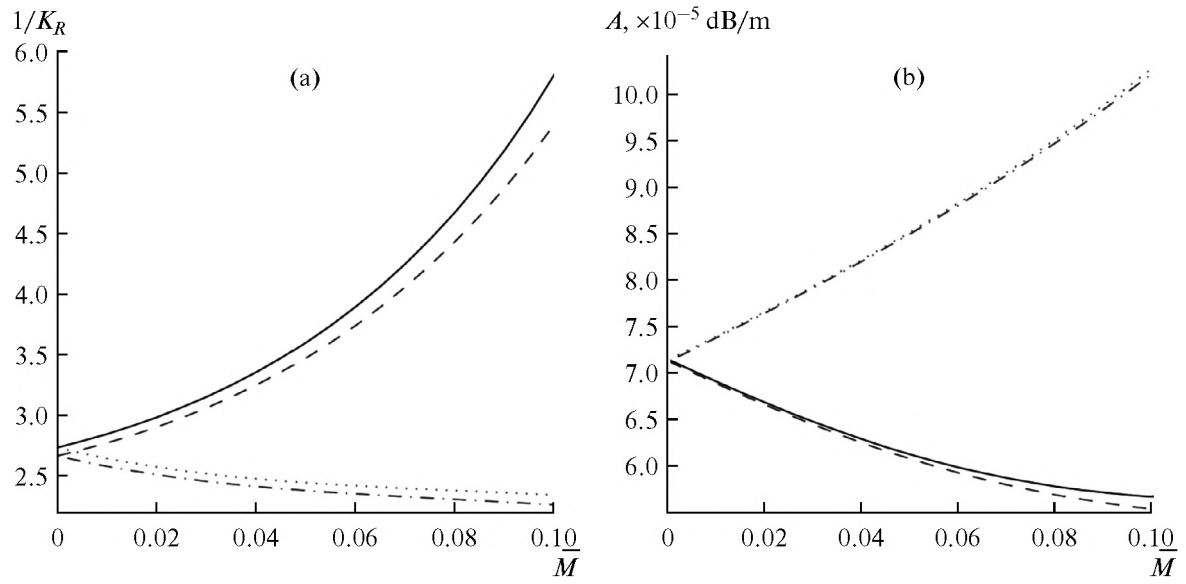

Fig. 2. The effect of flow profile on the relative phase velocity and attenuation coefficient of the second non-isentropic and isentropic acoustic waves propagating in a tube filled with water. (a) relative phase velocity; (b) attenuation coefficient. The legends are placed in Fig. 1a.

dimensionless wavenumber K. Similar manipulations can be found in Chen et al. [21] and Sobolev [6].

The Case of Liquid

Figure 1 respectively demonstrates the relative phase velocity (defined by $1/K_R$) and attenuation coefficient (defined by $A = |8.686k_0K_I|$ [dB/m]) of the first mode, while Fig. 2 shows the features of the second mode. Particularly, the characteristics of the non-isentropic and isentropic acoustic waves propagating forwardly and backwardly are compared. The legends of these figures are displayed in Fig. 2a. Specifically, "non-isentropic" and "isentropic" represent that the numerical results are calculated from the non-isentropic acoustic and isentropic models respectively; "down" and "up" show the downstream and upstream propagation.

Under the presence of a steady flow, the relative phase velocity in the downstream propagation is amplified compared with the case of the stationary fluid ($\overline{M} = 0$). Meanwhile, the attenuation coefficient decreases as the process of viscous friction becomes short. On the other hand, the steady flow inhibits the backward acoustic wave propagating in the fluid. The thermoviscous dissipation then becomes large, leading to an increase of the attenuation coefficient.

Compared with the first mode, the influence of the steady flow on the second mode is more complicated as shown in Fig. 2. Furthermore, with the increase of the mean Mach number, the difference between the non-isentropic and isentropic acoustic waves in the downstream propagation shows obvious. For each mode, the relative phase velocity of the non-isentropic acoustic wave turns out to be larger than that of the isentropic simplification. On the other hand, variation of the attenuation coefficient is different between the two modes. Further discussions are placed in the following subsection.

The Case of Gas

Figure 3 respectively demonstrates the relative phase velocity and attenuation coefficient of the first mode, while Fig. 4 shows the features of the second mode. Particularly, the characteristics of the non-isentropic and isentropic acoustic waves propagating forwardly and backwardly are compared. The legends of these figures are displayed in Fig. 2a. Obviously, the difference between the non-isentropic and isentropic acoustic waves is extremely distinct, which reveals that the energy transformation through the process of thermal conduction is more important in the case of perfect gas than that in the case of water.

While the tendency of the relative phase velocity as a function of the mean Mach number behaves similar in the perfect gas and water, the attenuation coefficient in the perfect gas is distinct from that in water. For the first mode, the attenuation coefficient in the downstream propagation decreases against the mean Mach number in water while the attenuation coefficient in the perfect gas increases. The behavior of the attenuation coefficient of the upstream propagation shows more complicated in the perfect gas.

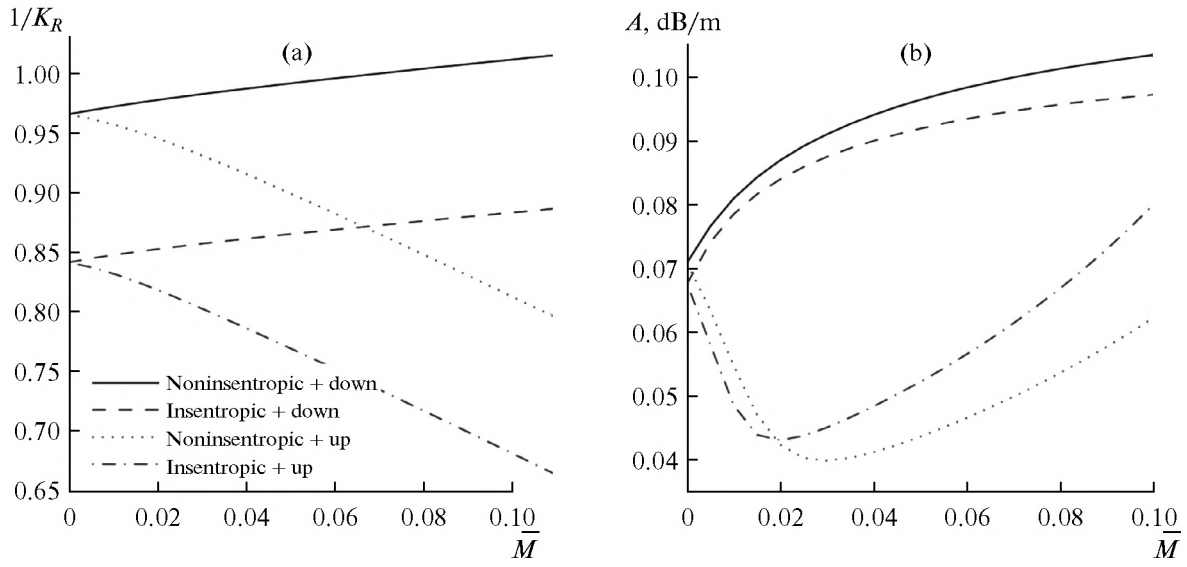

Fig. 3. The effect of flow profile on the relative phase velocity and attenuation coefficient of the fundamental non-isentropic and isentropic acoustic waves propagating in a tube filled with perfect gas. (a) relative phase velocity; (b) attenuation coefficient. The legends are placed in Fig. 3a.

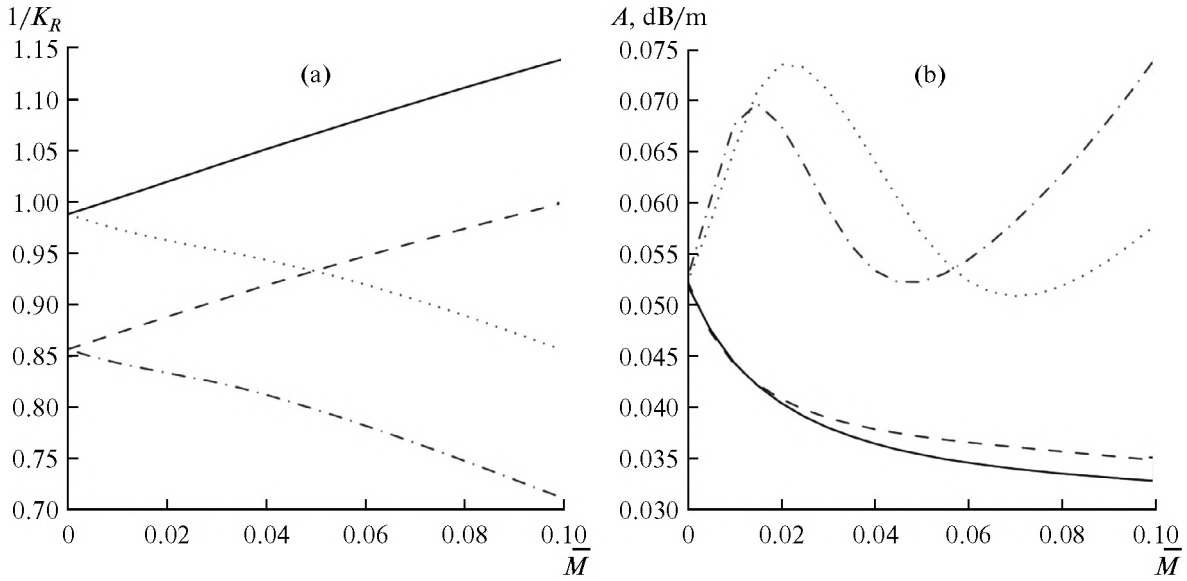

Fig. 4. The effect of flow profile on the relative phase velocity and attenuation coefficient of the second non-isentropic and isentropic acoustic waves propagating in a tube filled with perfect gas. (a) relative phase velocity; (b) attenuation coefficient. The legends are placed in Fig. 3a.

Physically speaking, without the presence of a moving flow, an acoustic wave can disturb the fluid particles, which brings about viscous friction between the particles. The vibration energy of an acoustic wave then transforms to the internal heat. In the presence of a shear flow, the shear force amplifies the energy dissipation of wave. An increase of attenuation coefficient in the downstream propagation as shown in Figure 3b reveals that the shear force regulates the first mode into a layer near the pipeline wall where the shear force is the largest over the pipeline radius. As a result, the corresponding attenuation coefficient goes up. On the other hand, the shear force channels the backward acoustic wave to the layer near the pipeline center where the shear force is the smallest. The energy dissipation then becomes slight. However, the existence of the flow slows down the propagation speed and then finally enlarges the attenuation coefficient.

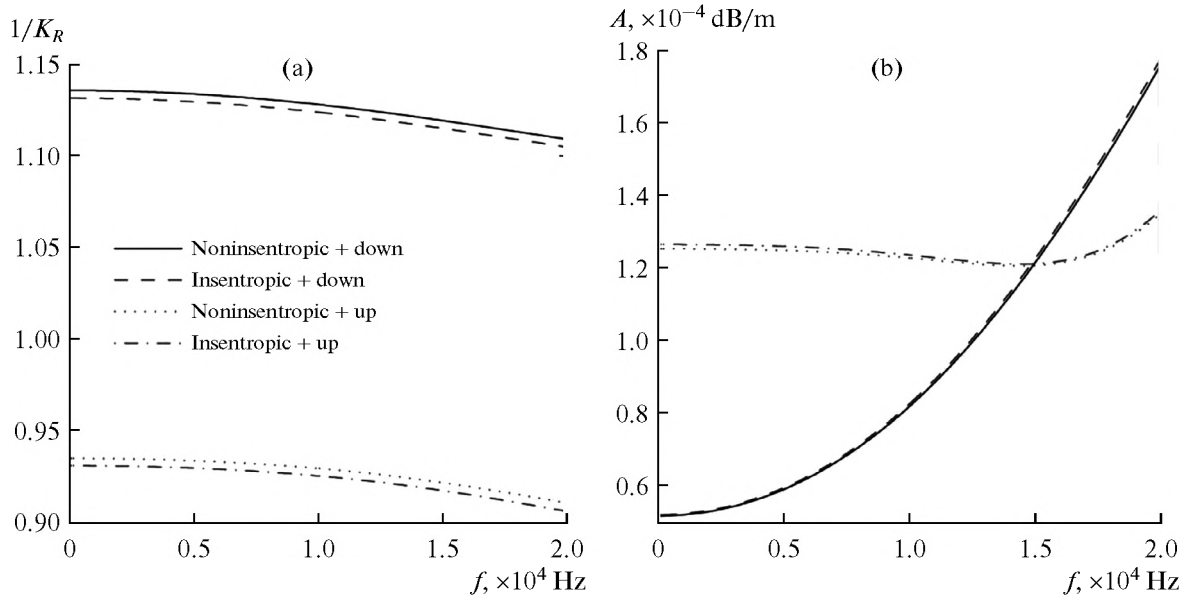

Fig. 5. The effect of acoustic frequency on the relative phase velocity and attenuation coefficient of the fundamental non-isentropic and isentropic acoustic waves propagating in a tube filled with water. (a) relative phase velocity; (b) attenuation coefficient. The legends are placed in Fig. 5a.

A possible problem can be that why the trends of the attenuation coefficients between water and perfect gas are distinctly different under the same configuration of the acoustic frequency, pipeline radius and flow profile. A possible explanation may be that the wavelength of the acoustic wave in water is larger than that in the perfect gas under the same acoustic frequency. The effect of the shear force on the acoustic wave with a smaller wavelength is easier than that with a larger wavelength.

The tendency of the attenuation coefficient of the second mode in the downstream propagation as shown in Fig. 4b behaves similar to the case of water as shown in Fig. 2b. However, change of the attenuation coefficient in the upstream propagation is more complicated than that in water. Initially, the increasing of the mean Mach number decelerates the backward propagation, leading to an increment of the attenuation coefficient. Meanwhile, the influence of the shear force also adds contributions to the increment of the attenuation coefficient. When the shear force is so big that the corresponding attenuation coefficient decreases, the total attenuation coefficient begins to decrease.

THE EFFECT OF ACOUSTIC FREQUENCY

This section analyzes the effect of the acoustic frequency on the first two modes in the presence of the laminar flow with the mean Mach number $M = 0.1$ while other parameters are the same as listed in the previous section.

The Case of Liquid

Figure 5 shows the effect of the acoustic frequency on the features of first mode while Fig. 6 plots the features of the second mode influenced by the acoustic frequency. With the increase of the acoustic frequency, the difference of the features between the non-isentropic and isentropic acoustic models is not distinct. Furthermore, the relative phase velocity of each mode gradually goes down to converge as the acoustic frequency goes up.

As the acoustic frequency climbs, the attenuation coefficient of the forward wave quickly ascends without a limit as shown in Fig. 5b. However, the attenuation coefficient of the backward wave slowly goes up and surpasses that of the forward wave. As explained in the previous section, the increase of the acoustic frequency leads to a decrease of the acoustic wavelength. The effect of shear force can more easily channel the acoustic wave which has shorter wavelength to the pipeline center in the downstream propagation and to the pipeline wall in the upstream propagation.

The tendency of the attenuation coefficient of the second mode in Fig. 6b with respect to the acoustic frequency is different from the first mode in Fig. 5b. With the increase of the acoustic frequency, the attenuation coefficient of the upstream propagation goes up more quickly than that of the downstream propagation. It can be learned that the effects of acoustic frequency and flow profile on the acoustic wave are dependent.

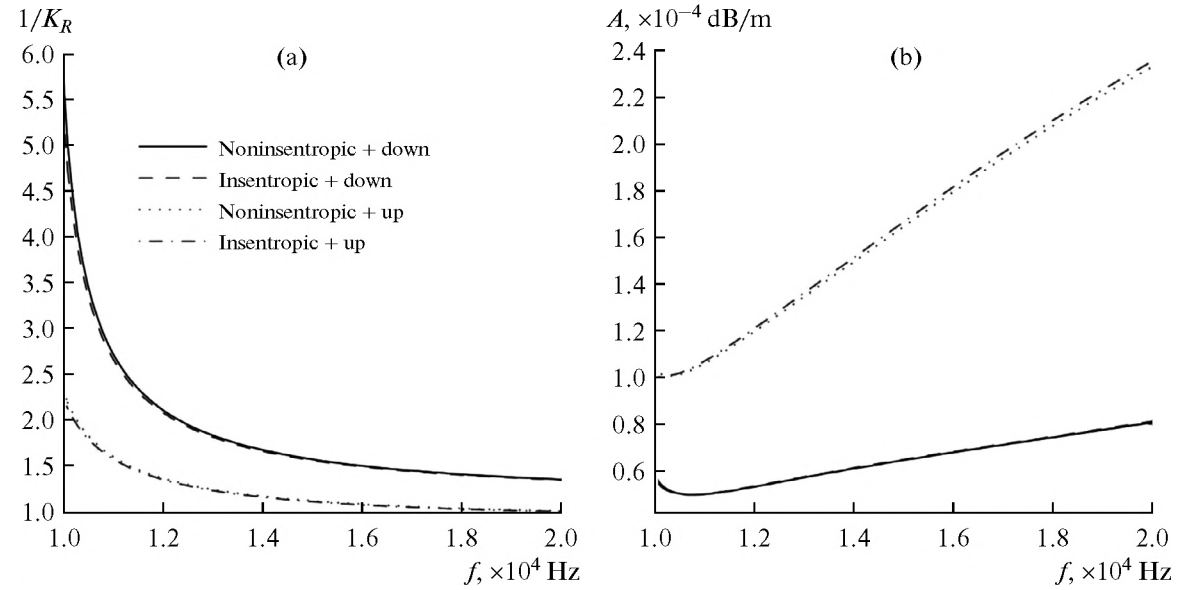

Fig. 6. The effect of acoustic frequency on the relative phase velocity and attenuation coefficient of the second non-isentropic and isentropic acoustic waves propagating in a tube filled with water. (a) relative phase velocity; (b) attenuation coefficient. The legends are placed in Fig. 6a.

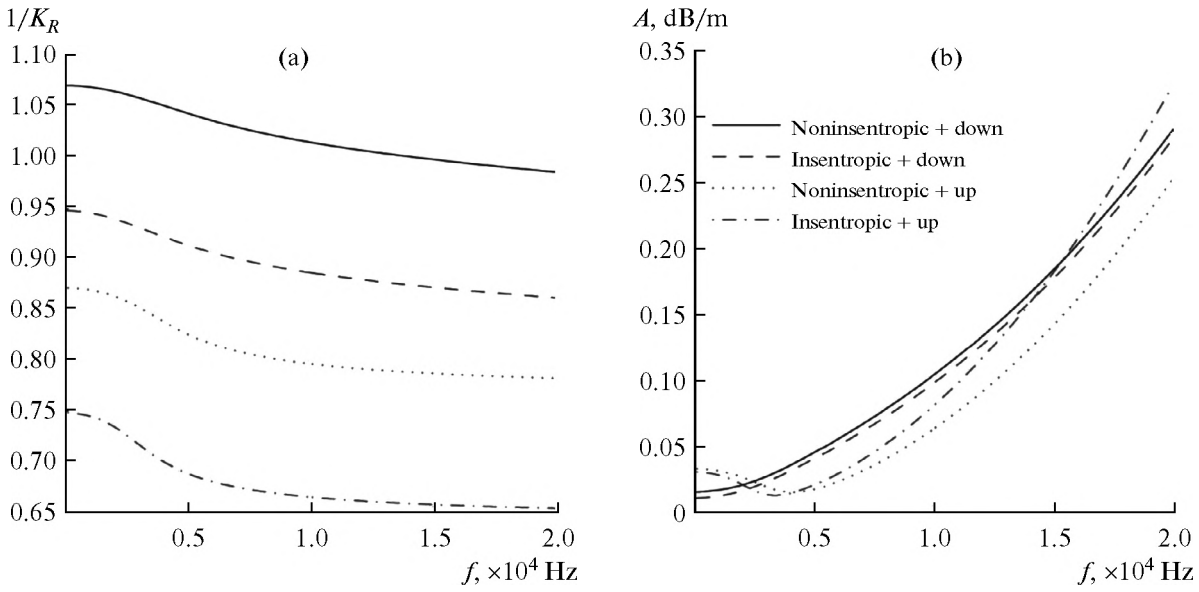

Fig. 7. The effect of acoustic frequency on the relative phase velocity and attenuation coefficient of the fundamental non-isentropic and isentropic acoustic waves propagating in a tube filled with perfect gas. (a) relative phase velocity; (b) attenuation coefficient. The legends are placed in Fig. 7b.

The Case of Gas

Figure 7 shows the effect of the acoustic frequency on the features of first mode while Fig. 8 plots the features of the second mode influenced by the acoustic frequency. The legends of the figures in Figs. 7 and 8 are identical to that in Fig. 6. Clearly, the tendency of the relative phase velocity of each mode in the perfect gas is similar to that in water. As the wavelength of the acoustic wave in the perfect gas is smaller than that in water, the influence of the shear force is more powerful. From Fig. 7b, it can be learned that the attenuation coefficient of the backward wave finally overtakes the attenuation coefficient of the forward wave in the case of a large frequency, which shows that the viscous dissipation behaves differently when the configurations of acoustic frequency and flow profile changes.

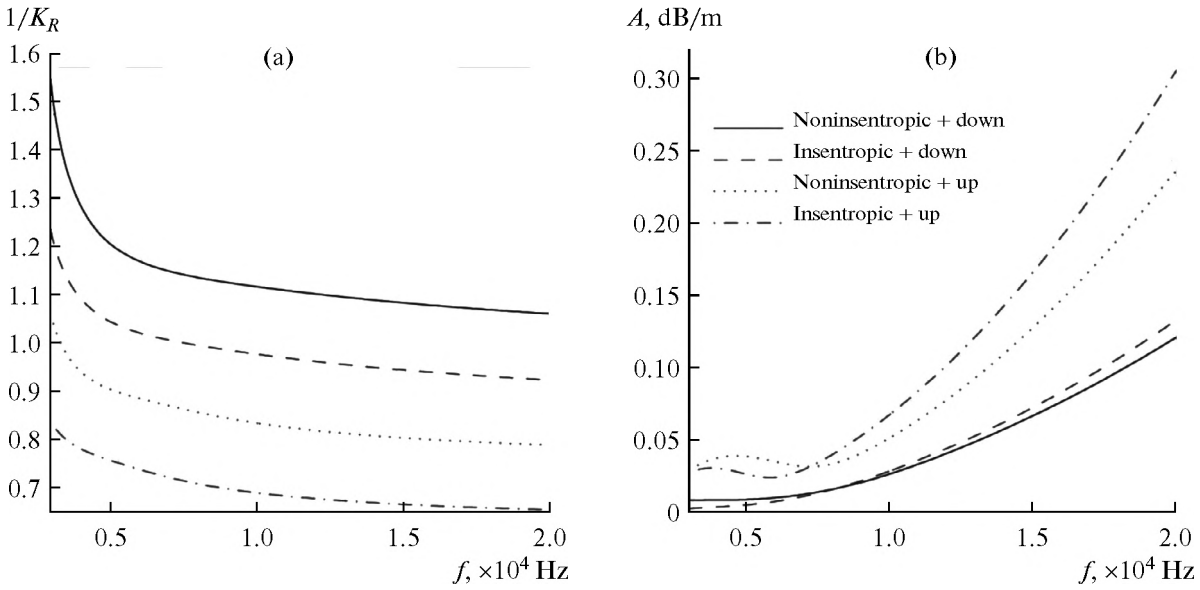

Fig. 8. The effect of acoustic frequency on the relative phase velocity and attenuation coefficient of the second non-isentropic and isentropic acoustic waves propagating in a tube filled with perfect gas. (a) relative phase velocity; (b) attenuation coefficient. The legends are placed in Fig. 8b.

In the case of a low acoustic frequency, the difference of the attenuation coefficients between the non-isentropic and isentropic acoustic models is slight. However, with the increase of the acoustic frequency, the difference becomes obvious especially in the upstream propagation. The effect of a steady flow also has similar tendency as shown in Figs. 3b and 4b. Compared with non-isentropic acoustic wave, the attenuation coefficient of the isentropic wave behaves more sensitive to the acoustic frequency as well as the flow profile, except the first forward mode. It reveals that the thermal conduction plays an important role in the wave propagation along the perfect gas.

CONCLUSIONS

This paper numerically analyzes the features (relative phase velocity and attenuation coefficient) of the first two axisymmetric acoustic modes propagating forwardly and backwardly along the laminar flow confined by a circular rigid wall. Parametric analysis of the effects of the flow Mach number and the acoustic frequency are addressed in liquid and perfect gas respectively. Meanwhile, the influence of thermoviscous dissipation is demonstrated. Numerical comparisons reveal that:

1—Although the isentropic acoustic model may be a reasonable alternative to the non-isentropic model in liquid, the difference between the two models may be amplified if acoustic frequency and steady flow Mach number becomes large. On the other hand, the isentropic acoustic model may be controversial in the case of the perfect gas.

2—The shear effect greatly changes the features of the acoustic wave propagating backwardly and forwardly. Such influence is extremely obvious when the acoustic wavelength is short.

3—The effects of the shear flow and acoustic frequency act independently on the acoustic wave. To get a highly accurate prediction, these factors must be considered coherently in the mathematical modeling.

The work described in this paper is funded by the National Natural Science Foundation of China (Nos. 11404405, 91216201, 51205403 and 11302253). The authors gratefully acknowledge the funding.

REFERENCES

1. V. M. Butorin, Acoust. Phys. **59**, 625 (2013).
2. A. Gupta, K.-M. Lim, and C. C. Heng, Acoust. Phys. **59**, 493 (2013).
3. A. I. Komkin, M. A. Mironov, and S. I. Yudin, Acoust. Phys. **60**, 145 (2014).
4. V. F. Kovalev and O. V. Rudenko, Acoust. Phys. **58**, 269 (2012).
5. A. A. Osipov and K. S. Reent, Acoust. Phys. **58**, 467 (2012).
6. A. F. Sobolev, Acoust. Phys. **58**, 490 (2012).
7. E. J. Brambley, A. M. J. Davis, and N. Peake, J. Fluid Mech. **690**, 399 (2012).
8. V. F. Kopiev, M. Y. Zaytsev, and N. N. Ostrikov, Acoust. Phys. **59**, 207 (2013).
9. V. F. Kopiev, I. V. Belyaev, M. Y. Zaytsev, V. A. Kopiev, and G. A. Faranosov, Acoust. Phys. **59**, 19 (2013).

10. Y. D. Khaletskiy, Acoust. Phys. **58**, 556 (2012).
11. B. M. Efimtsov and L. A. Lazarev, Acoust. Phys. **58**, 443 (2012).
12. G. I. Broman and O. V. Rudenko, Acoust. Phys. **58**, 537 (2012).
13. I. V. Belyaev, Acoust. Phys. **58**, 387 (2012).
14. K. S. Peat, J. Sound Vib. **175**, 475 (1994).
15. K. S. Peat and R. Kirby, J. Acoust. Soc. Am. **107**, 1859 (2000).
16. Y. Chen, Y. Huang, and X. Chen, J. Acoust. Soc. Am. **134**, 1863 (2013).
17. Y. Chen, Y. Huang, and X. Chen, Acta Acust. Acust. **99**, 875 (2013).
18. Y. Chen, X. Chen, Y. Huang, Y. Bai, D. Hu, and S. Fei, Acoust. Phys. **62**, (2016) [in print].
19. Y. Chen, Y. Huang, X. Chen, and D. Hu, J. Comput. Acoust. **22**, 1450014 (2014).
20. R. Boucheron, H. Bailliet, and J.-C. Valiere, J. Sound Vib. **292**, 504 (2006).
21. Y. Chen, Y. Huang, and X. Chen, J. Acoust. Soc. Am. **134**, 2619 (2013).